RSC Advances

PAPER

View Article Online
View Journal | View Issue

Cite this: *RSC Adv.*, 2017, **7**, 14159

Rapid synthesis for monodispersed gold nanoparticles in kaempferol and anti-leishmanial efficacy against wild and drug resistant strains

Asim Halder,[a] Suvadra Das,[a] Tanmoy Bera[b] and Arup Mukherjee*[a]

Received 23rd December 2016
Accepted 17th February 2017

DOI: 10.1039/c6ra28632a

rsc.li/rsc-advances

Leishmaniasis is a WHO notified neglected tropical disease (NTD) caused by the *Leishmania* parasite species. The parasite locates rapidly in the macrophage cells and survives there for a long period of time with or without any symptomatic response. Eliminating Leishmania from the macrophage sites is complicated. Only a few antileishmanial drugs are known and most of them have developed resistance over the time. We have synthesized highly monodispersed gold nanoparticles (KAunp) in a rapid reduction reaction catalyzed in kaempferol. Kaempferol stabilized nanoparticles in 18.24 nm size domain were used as leishmanicidals in macrophage infested conditions. KAunps' CC_{50} in the macrophages was at 2.4×10^2 μM while that for sodium stibogluconate was 27 μM. Phagocytic uptake in infested cells was fast and remarkable. KAunps were explicitly effective against both the wild and drug resistant organisms. Monodispersed gold nanoparticles synthesized in green technology appeared as safer alternatives for leishmanial chemotherapy.

1. Introduction

Gold nanoparticles are veritable tools for applications in the chemical biology interfaces.[1] Particle parameters like the size, morphology, scaffolding, surface charge and dispersity are some of the very crucial parameters for successes in biology. Nanoscale surface chemistry and particle aspect ratio for example influences cellular trafficking.[2,3] In sharp contrast to the soft polymer nanoparticles, inflexible nanocarriers like the metal and metal oxides face much faster uptake in infected cell targets.[4,5] Gold nanoparticles near spherical were apparently safe and elicit low or no systemic immunity reactions. Furthermore, particles in sub 100 nm ranges were encouragingly effective in cancer chemotherapy and microbial infection control.[6,7] Nanoparticles by design were also projected as one successful strategy against complex immune cell resident infections like that in HIV aids and tuberculosis.[8–10] We postulated that flavonoid stabilized spherical gold nanoparticles may provide some useful tools for precise control of macrophage resident leishmania infections.

Synthesis of gold nanoparticles typically involved reduction of tetrachloroauric acid in sodium borohydride or sodium citrate. Unfortunately, the temperature dependent citrate method produced quality particles only up to ~50 nm in size and beyond which they are polydispersed and nonspherical.[11] Sodium borohydride reduction is very fast and particle uniformity is always affected. Various green techniques for nano-gold synthesis and *in situ* functionalization were experimented.[12] Inconsistent particle characteristics reported in similar conditions was mostly due to sluggish redox reactions. Reducing gold onto seeds prior to the growth steps is perhaps a practicable strategy for consistent nanoparticle characteristics.[13] However, scale up synthesis and appropriate bio-molecular functionalizations were not often very feasible in similar techniques. Furthermore, reagents that are frequently used for gold nanoparticles stabilization are unsafe and not often biocompatible. For example, gold nanoparticles dispersion stability was often achieved with strongly bound toxic passivaters like CTAB (cetyltrimethylammonium bromide). Stable aqueous dispersion of uniform size gold nanocolloid carrying no toxic debris is nevertheless essential for therapeutic applications. Non-thermal gold nanoparticle synthesis and reliable particle quality for therapeutic application however remained elusive for a long time.

Leishmaniasis is a vector born neglected tropical disease (NTD). The disease is caused by *Leishmania* parasite species. The infection is endemic in different tropical regions. The organism is also known to migrate rapidly in war torn regions around the globe. The disease is now a major public health threat. Among all types, the visceral leishmaniasis (VL) caused by *Leishmania donovani* is life threatening and is most difficult one to be controlled. VL asymptotic infections are quite common which often surfaces later in immune compromise conditions like that in case of HIV-aids. Currently, there exists no perfect stratagem to contain similar infections in confinement. Once infested, the

[a]*Department of Chemical Technology, University of Calcutta, 92, A.P.C. Road, Kolkata-700 009, West Bengal, India. E-mail: arupm1234@gmail.com; Fax: +913323519755; Tel: +913323508387*

[b]*Department of Pharmaceutical Technology, Jadavpur University, 188 Raja S. C. Mullik Road, Kolkata-700 032, West Bengal, India*

parasite quickly locates themselves into phagocytic macrophage cells and employs biochemical strategies to survive and multiply.[14] Drug resistance is rampant and old drugs like sodium stibogluconate are no longer effective. Amphoterecin B (AmB) is effective but expresses a very narrow therapeutic window and is forbiddingly costly. Compounds like paromomycin or miltefosine are highly toxic and even teratogenic in some cases. Cross resistance in combination therapy is also very common.[15,16] Metal nanoparticles are explicitly experimented in therapeutics albeit a lot of incoherency in particle properties. Hard nanoparticles by design are also in high demand for infectious disease control and swift therapeutic delivery. Biosafe highly monodispersed noble metal nano-spheroids as drug carriers were considered as an early solution against immune cell resident infections.[17] This work was planned to address twine objectives of bio-safe gold nanoparticles synthesis in small size regime and containment of VL infections in microphage infested conditions. Antioxidant polyphenol kaempherol was used for the first time for uniform size gold nano-scaffolds synthesis in low temperature conditions. Kaempherol and the kaempherol stabilized nano-gold were used further as leishmanicidals in macrophage resident conditions.

2. Experimental

2.1. Materials

Chloroauic acid ($HAuCl_4 \cdot 3H_2O$), kaempferol, Amphotericin B (AmB) and RPMI-1640 cell culture medium were all purchased from Sigma-Aldrich (St. Louis, MO, USA). HPLC grade solvents and water were procured from E. Merck or Spectrochem (Mumbai, India). Sodium stibogluconate (SSG) was a kind gift from Albert David Ltd. (Kolkata, India). Standard glasswares of Borosil® (Mumbai, India) make were used for preparation and analysis experiments. All other reagents used were of analytical grade.

2.2. Synthesis of gold nanoparticles

Gold nanoparticles were synthesized under low temperature sonication in kaempferol. In a typical procedure, 3 ml of 1.0 mM chloroauric acid in water was added with 1 ml of 4 mM kaempferol and was vortexted to equilibrate. The reaction mixture was put to sonication for 1 min in a 50 Hz bath sonicator (UD 100SH-3L Takashi, Japan) maintained at 4 °C. KAunps were collected after centrifugation at 15 000 rpm for 30 min. The nanoparticles were washed in water, re-centrifuged and finally diluted in water and stored at 4 °C for further applications.

2.3. Characterization of nanoparticles

Formation of nanoparticles was confirmed by UV-vis spectral analysis. The plasmonic absorbances were monitored in a double beam UV-vis spectrophotometer (Shimadzu Japan-2550) at different reaction stages. The samples were diluted with water and absorption spectra were recorded at medium speed in the wavelength range of 200–800 nm. The particle size in hydrodynamics was monitored in a zetasizer Nano ZS (Malvern Instruments, Malvern, UK). A 4 mW He–Ne laser beam was used at 633 nm and back scattering angle of 173°. Particle polydispersity index (PDI) was recorded in the same instrument. Analysis experiments were conducted in triplicate for each sample batch and the results were reported as the mean ± standard deviation. Disposable zeta cells were used to measure particle electrophoretic mobility and Smoluchowski equation was applied for determining KAunp zeta potential (ζ) in water medium. A JEOL-JEM 2010 (JEOL, Tokyo, Japan) high-resolution transmission electron microscope (HR-TEM) operated at 200 kV and equipped with an energy-dispersive X-ray (EDAX) device was used to measure the size and homogeneity of the synthesized particles. Samples were prepared by applying 30 μl of diluted nanoparticle solution onto carbon-coated copper TEM grids (300 mesh, Ted pella, Redding, CA, USA). Excess solution was removed with a filter paper and the grids were allowed to dry prior to measurements. Approximately, 150 particles were counted and were measured for a size distribution study. Elemental analyses of the residues were carried out in EDAX analyzer attached to the TEM system. FT-IR studies were conducted over a wave number range of 4000 to 400 cm^{-1} in FT/IR-670 plus (Jasco, Tokyo, Japan) using DLATGS detectors. Pressed KBr disks were used at 4 cm^{-1} resolution. Both KAunp and kaempferol were studied and the data stacked in Bio-Rad KnowItAll (Bio-Rad, Hercules, CA) software for comparative analysis. X-ray diffraction analysis was performed on a Bruker AXS D8 (Bruker, Karlsruhe, Germany) diffractometer with Cu kα radiation ($\lambda = 1.5405$ Å) operated at an accelerating voltage of 40 kV and current intensity 40 mA. The scanning rate applied was 0.020 s^{-1} in the 2θ ranges of 30–80°. KAunp samples were digested in aqua regia for 2 h and Elan-DRC-e (Parkin Elmer, USA) ICPMS facility was used for Au analysis. Instrument operating conditions were 1050 Hz radio-frequency forward power, 12.8 l min^{-1} plasma carrier gas flow (argon), and 26 rpm nebulizer pump speed. Gold concentration was determined using Au^{197} isotope levels. Calibration curve was developed from the instrument standards in concentration range for 50 to 1000 ppb.

2.4. *In vitro* assessment of antileishmanial activity

2.4.1. Parasites and cell line. *L. donovani* promastigotes AG 83(MHOM/IN/1983/AG83), isolated from a 'kala-azar' patient was received as a gift from the Indian Institute of Chemical Biology, Council of Scientific and Industrial Research, Kolkata, India and used for experiments.[18] *L. donovani* amastigotes were grown and maintained in MAA/20 medium at pH 5.5 in 37 ± 2 °C incubator with 5% v/v CO_2/air mixture. In a span of 120 h promastigotes differentiated to amastigotes and cultures were maintained by dilutions once in a week. Mouse (swiss albino, female 22 ± 2 g) peritoneal macrophages were collected after 5 days of an i.p injection of 0.5 ml 4% thioglycollate broth. Exudate cells were harvested in RPMI-1640 medium supplemented with 2 g l^{-1} $NaHCO_3$, 10% fetal calf serum, 100 U ml^{-1} penicillin and 50 μg ml^{-1} streptomycin. After incubation for 2 h at 37 ± 2 °C, non-adherent cells were removed by thorough washing and adherent macrophages were cultured for 24 h at 37 ± 2 °C. Cultures prepared contained ≥95% of macrophages were evaluated by their ability to take up latex bead and by morphology. All animal studies were performed in compliance

with the guidelines of Committee for the Purpose of Control and Supervision of Experiments on Animals (CPCSEA), Government of India and the experimental protocols were approved by the institutional animal ethical committee (IAEC) of Jadavpur University (AEC/PHARM/1601/12/2016).

2.4.2. Macrophage infested resistant amastigote. Resistance development in *L. donovani* AG83 promastigotes were first performed by addition of SSG or paromomycin (PMM) in the growth medium at an increasing concentration.[19] Promastigotes in the logarithmic growth phase were cultured continuously at a particular drug concentration which killed 90 to 95% of the parasites exposed. Surviving subpopulation of parasites that were stabilized to grow successfully in new drug concentration was further exposed to subsequent higher concentrations of SSG or PMM. Drug resistant phenotypes were differentiated into amastigotes within 120 h of growth in MMA/20 medium at pH 5.5 placed in a 5% v/v CO_2/air mixture and 37 ± 2 °C at incubator.

2.4.3. Anti-leishmanial assay *in vitro*. Anti-amastigote activities were studied by direct counting growth inhibition assay with slight modifications.[20] Amastigotes were seeded at an initial concentration equivalent to early log phase (3×10^5 amastigotes per ml) and multiplied for 72 h either in the medium alone or in presence of serial dilution of the test compound until the late log phase (1×10^6 cells per ml). Axenic amastigote number doubled three to four times during the assay in maintenance media. IC_{50} (50% inhibitory concentration) for each test compound was determined in parallel. The amastigotes were counted using hemocytometer slides under a microscope. All experiments were done in triplicate for comparative purposes.

2.4.4. Anti-amastigotes activity in macrophage. Susceptibility of *L. donovani* amastigotes in macrophages was evaluated as proposed by Chang *et al*. with minor modification.[21] Briefly macrophages were seeded in α-10 medium at 4×10^4 cells per well count in chamber slides and kept for 24 h at 37 ± 2 °C for attachments. Macrophages were infected to axenic amastigotes (4×10^5 amastigotes per well) for 4 h at 37 ± 2 °C. To remove non-phagocytosed parasites slides were washed with Dulbecco's phosphate-buffer saline. Standard drug and test compounds were dissolved in culture medium and incubated with different concentrations for 72 h at 37 ± 2 °C in a 5% v/v CO_2/air mixture in incubator. Treatment solutions and the medium were replaced with fresh ones every 24 h. Control wells of the infected macrophages were incubated with the same medium. Activity in each case was estimated from the percentage reduction in amastigote number in treated and untreated cultures. Observation were recorded in methanol-fixed, giemsa stained (10% v/v) preparations. The antileishmanial effects were expressed as IC_{50} values and the results were averaged in each concentration from triplicate observations.

2.5. Cytotoxicity studies against mammalian macrophages

Macrophage cells were cultured in minimum essential medium (MEM, Gibco), supplemented with 20 mM L-glutamate, 16 mM $NaHCO_3$, 5% fecal calf serum and penicillin–streptomycin. The assay was performed in 96-well tissue culture plates in presence of standard counts of the macrophages. The wells were seeded with test solutions in different dilution and the viable macrophages were counted microscopically after 48 h of exposure at 37 ± 2 °C in a 5% v/v CO_2 incubator.

2.6. Nanoparticle macrophage uptake studies in TEM

The cellular uptake of KAunps into macrophage cells was observed in TEM (FP 5018/40 (TECHNAI G^2 SPIRIT BioTWIN, Czech Republic). Macrophage cells were cultured on 6 well tissue culture plates and incubated overnight for growth under 5% CO_2 at 37 ± 2 °C. In the next day, growth plates were exposed to 10 μM KAunp concentration for different time periods (10 min, 30 min, 1 h and 2 h). Cells after exposure were washed with 0.1 M PBS and pellets were spun at 3000 rpm for 10 min. Washed cells were collected after three similar repeat centrifugations and were fixed in a mixture of 2% paraformaldehyde and 2.5% glutaraldehyde in 0.1 M PBS for 2 h.[22] Fixed samples were washed and stained with 1% osmium tetra oxide at 4 °C for observations. Cell pellet dehydration was performed in graded concentration of acetone (30, 50, 70, 90, and 100%) followed by toluene. Samples were subsequently embedded in epoxy resin and cut into 80 nm thin sections and analyzed in TEM at 75 kV.

2.7. Statistical analysis

Data collected were expressed as the mean ± standard deviation. Biological analysis data were gathered in triplicates and were assessed following Student's *t* test. Statistical significance was recorded when $p < 0.05$.

3. Results and discussion

3.1. Gold nanoparticle synthesis

The size and purity of gold nanoparticles in *ab initio* synthesis depends generally on nucleus formation reduction rate, and subsequent molecular association. Turkevich originally reported citrate stabilized ~20 nm gold nanoparticles synthesis in water.[13] Particle size control by varying reagent ratio was later achieved and the reduction kinetics studied by different researchers.[11,12,23,24] In our case gold nanoparticles were synthesized by reducing $HAuCl_4$ with kaempferol under ultrasound in low bath temperature conditions. The polyphenolic compound kaempferol is a powerful reducing agent (reduction potential 0.98 V).[25] Fast reduction of $HAuCl_4$ under constant frequency ultrasound at 4 °C was presented in Fig. 1. The solution color changed from pale yellow to violet within 15 s. Plasmonic intensity at 541 nm gained rapidly thereafter and a saturation point was achieved within 1 min. Fern's nucleation-diffusion and growth mechanism appeared responsible for nanoparticles synthesis in low temperature ultrasound conditions.[26] This reaction when monitored at different time points the plasmonic peak was always recorded at 541 nm up to 1 min of reaction time (Fig. 2A). Beyond that time the peak intensity was reduced and a peak shift was observed due to particle aggregation and irregular formations (Fig. 2B). The plasmonic absorbance peak decreased when the reactive molar

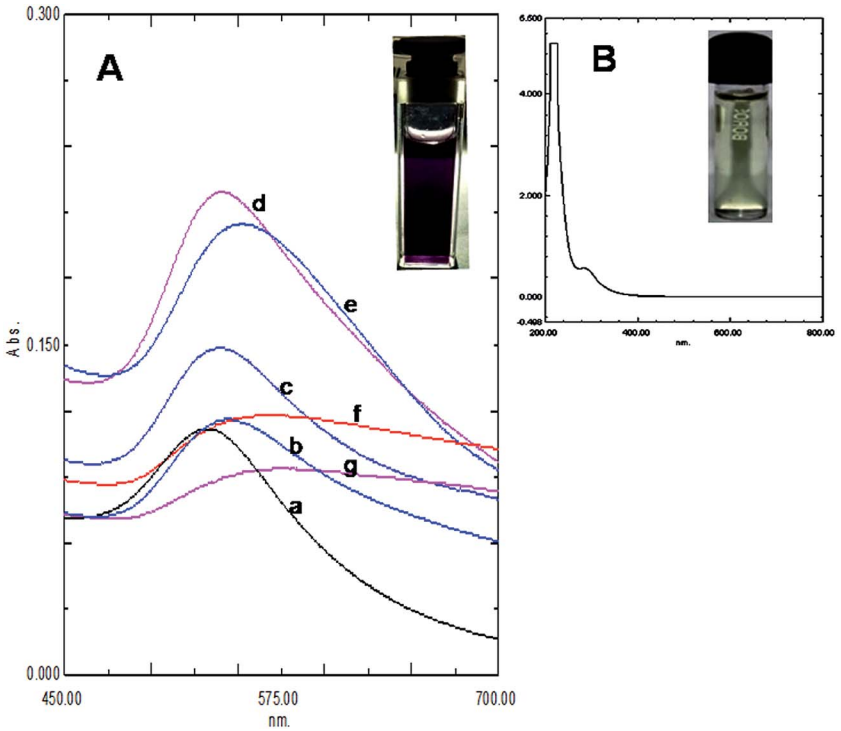

Fig. 1 (A) UV-vis spectra of gold nanoparticles prepared in different molar proportion of kaempferol and gold chloride: (a) 1 : 1, (b) 2 : 1, (c) 3 : 1, (d) 4 : 1, (e) 5 : 1, (f) 6 : 1and (g) 7 : 1. (B) UV-vis spectra of $HAuCl_4$ aqueous solution. Inset images taken from aqueous gold salt solution (inset B) and gold nanoparticles (inset A).

concentration was adjusted to the lower ratios (4 : 1 > 3 : 1 > 2 : 1 > 1 : 1). The peak responsible for the aqueous gold salt solution (Fig. 1B) disappeared completely and the intense violet color fixed peak due to KAunp soon appeared (Fig. 1A). The flavonoid kaempherol and chloroauric acid molar ratio for ultrasound reduction reaction was therefore set at 4 : 1. When $HAuCl_4$ was exposed to kaempferol without sonication no color change was recorded even after 2 h of observation period (Fig. 2A inset). The Au^{3+} Au^0 standard reduction potential is ~1.0 V.[27] At low temperature conditions kaempherol only has failed to initiate Au nuclear transformations. In conducting medium like water ultrasound is known to create pressure waves and induce molecular vibrational motions. Ultrasound compression waves generate cavities consecutively inside the bulk medium. Short lived water bubbles developed due to cavitational effects expanded under negative pressure excursion

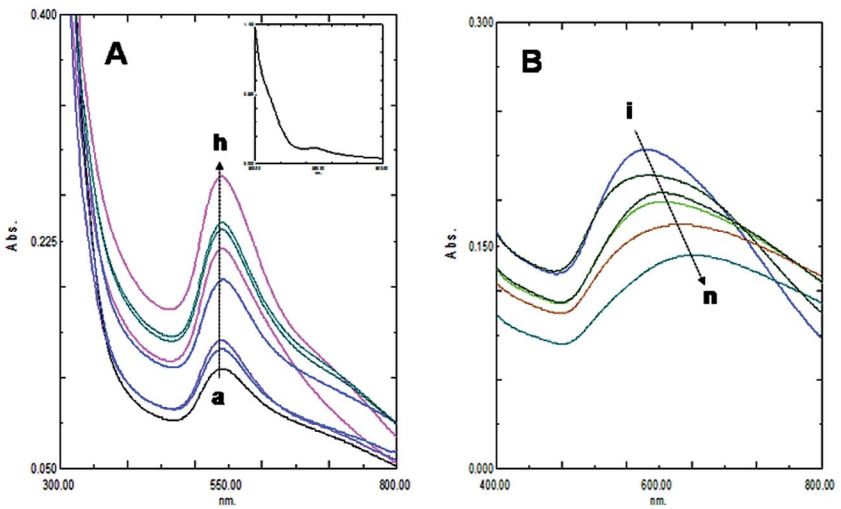

Fig. 2 UV-vis spectra obtain from different time point of reaction: (A) spectra recorded at (a) 5 s, (b)10 s, (c)15 s, (d) 20 s, (e) 30 s, (f) 40 s, (g) 50 s and (h) 60 s. inset figure, UV-vis spectra recorded without sonication. (B) spectra recorded at (i) 70 s, (j) 80 s, (k) 90 s, (l) 100 s, (m) 110 s and (n) 120 s.

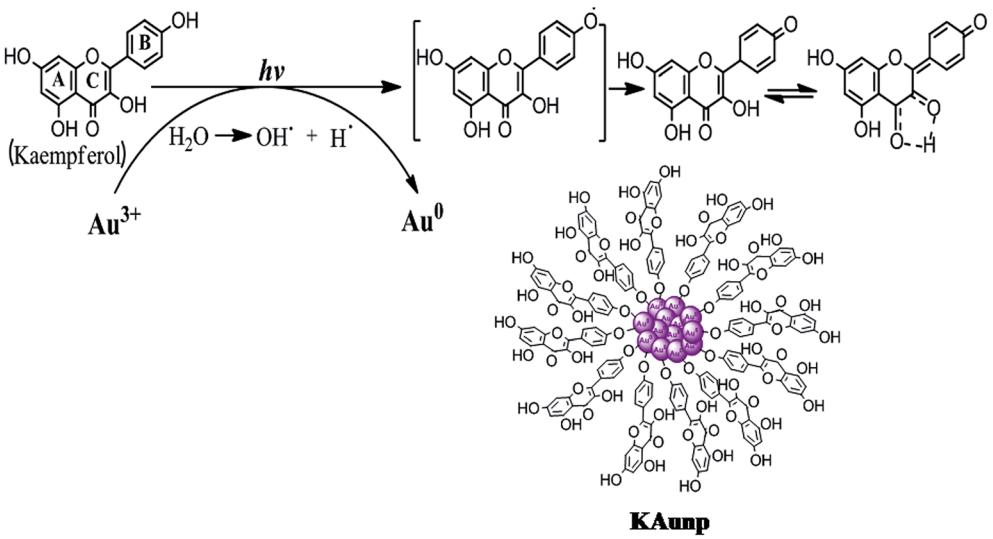

Scheme 1 Schematic diagram showing possible mechanism of gold nanoparticles formation and stabilization in kaempferol under sonication.

and crush very fast. The energy release per minute due to cavitational implodes in bubble centers is extremely high.[28] The energy exposure on kaempferol molecules under ultrasound has thus enabled a rapid reduction, gold nucleation and highly monodispersed nanoparticles formations. When ultrasound induced reduction reaction was continued beyond 1 min gold nanoparticles faced enhanced cavitational collapse, fast collision and likely overgrowth.

Kaempferol is a flavonoid with highest antioxidant capacity among all plant polyphenolic compounds. The hydroxyl group in flavonoid ring B played an important role in the hydrogen atom transfer reactions.[29] The rate of reaction in kaempferol with one hydroxyl group in ring B was faster than quercetin having 3′,4′-OH groups. Furthermore, the 3-OH substitution in the ring C and the torsion angle for ring B and C provided a crucial stability parameter for the kaempferol free radical. The

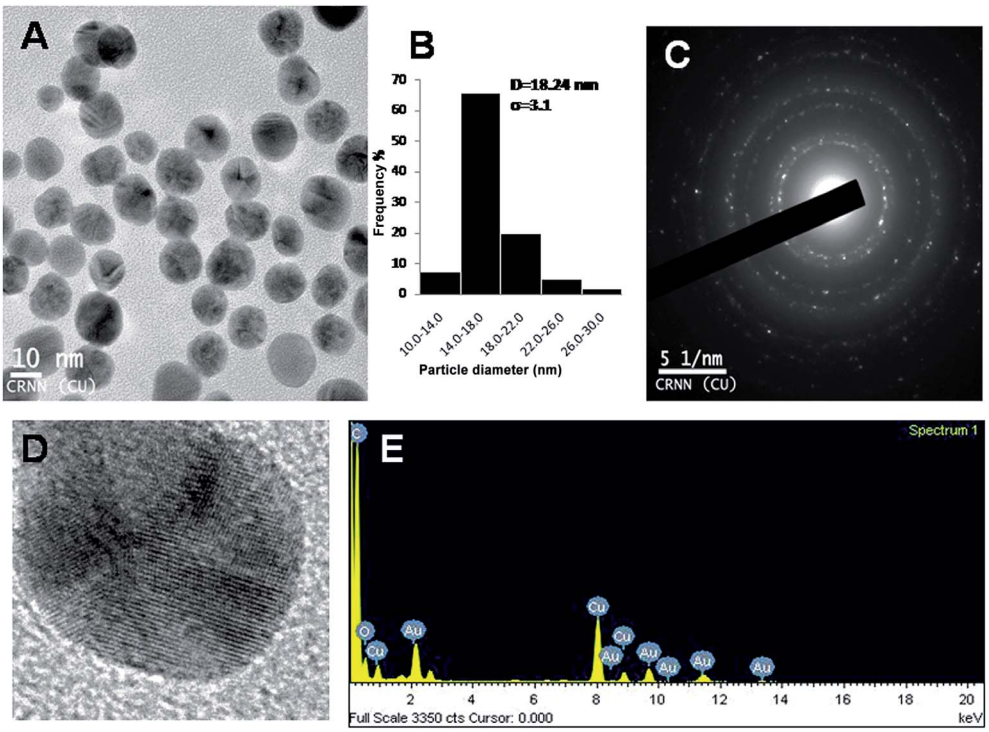

Fig. 3 (A) TEM study of KAunp. (B) KAunp size distribution histogram. (C) SAED pattern. (D) High resolution image of single nanoparticle. (E) EDAX spectrum of KAunp.

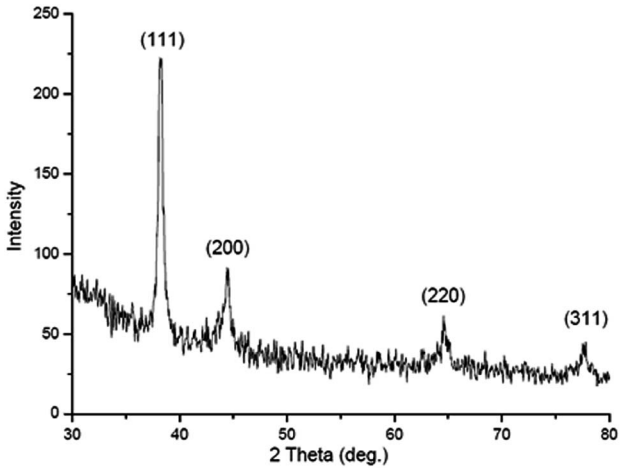

Fig. 4 XRD spectrum of KAunp.

compound therefore takes a *p*-quinone methide structure upon ultrasound facilitated H atom abstraction (Scheme 1).

3.2. Particle characterization

The hydrodynamic radii of KAunps were recorded in DLS. The average diameter in hydrodynamics was at 120 nm and the PDI was at 0.127 indicating, particle uniformity and monodispersion. The zeta potential was recorded at −21.2 mV which was likely due to stabilizing molecules presence in the vicinity. The HRTEM images and size distribution for typical KAunps were shown in Fig. 3. It was clear that the nanoparticles were spherical with no obvious agglomeration. The size distribution histograms were developed from 150 particle counts from three different TEM zone studies (Fig. 3B). The average particle size observed in HRTEM was 18.24 ± 3.1 nm. The EDAX observations indicated gold atoms encompassed with oxygen. Fig. 3C presented KAunp selected area electron diffraction (SAED) studies. Gold crystal growth lattice planes with lattice fringe spacing were recorded at 0.156 nm. The XRD observations were presented in Fig. 4. The diffraction peaks were indexed for (1 1 1), (2 0 0), (2 2 0) and (3 1 1) reflections due to face centered cubic (fcc) structure formations. ICPMS analysis of the final KAunps in water confirmed Au concentration at 174 μg ml^{-1} Au.

KAunps structure and formations during the reaction time course were also studied in HRTEM (Fig. 5). Samples were withdrawn at different time points, diluted in 50% v/v ethanol–water at 0 °C and drop cast on TEM grids before imaging. At the initial stages (upto 15 s) particles appeared as aggregates or very small in size (<7 nm) and agglomerates. Small size particles disappeared or possibly re-dissolved and relatively larger aggregates were recorded near 25 s reaction time. Nanoparticle size and shape uniformity was always clear when samples were studied in 60 s of reaction time. Aggregates were disappeared and particle size stabilized at near uniform 18.24 nm. TEM findings suggested that the growth of the nanoparticles possibly followed gold atomic deposition on the surface rather than forming compact aggregates.[24]

The FT-IR spectra were recorded to find out kaempferol interactions with the gold nanoparticles (Fig. 6). The native kaempferol showed characteristic broad band at 3309 cm^{-1} corresponding to the phenolic OH. Another band observed at 1659 cm^{-1} was assigned for stretching vibration of C=O groups in C ring of the flavonoid structure.[30] The band observed at 1048 cm^{-1} corresponded to the benzopyran group and several stretching bands around 1607, 1503, 1448 cm^{-1} were due to the aromatic skeleton. In case of KAunp the characteristic O–H stretching vibrations decreased in intensity and sifted to 3396 cm^{-1}. Absorption peaks due to the benzopyran group remained

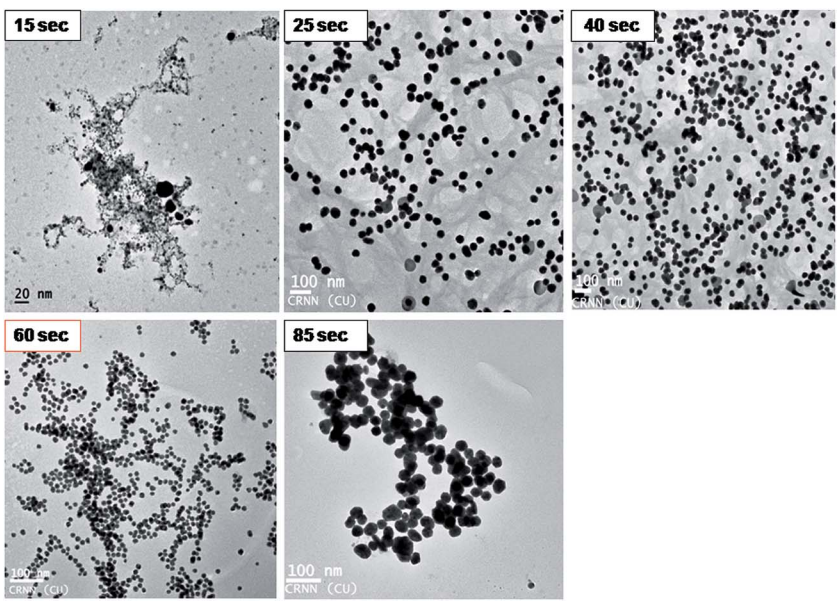

Fig. 5 HRTEM images of KAunps obtained after 15 s, 25 s, 40 s, 60 s and 85 s of reaction.

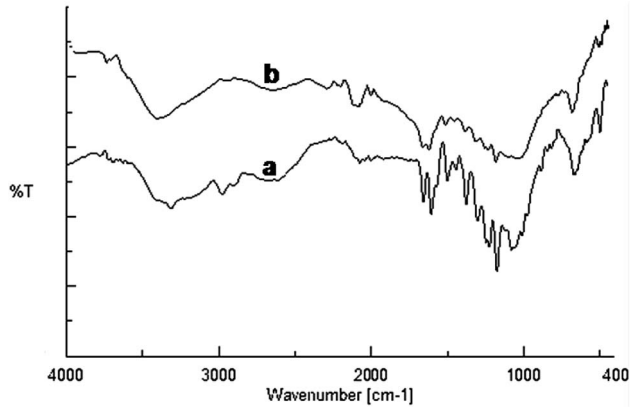

Fig. 6 FTIR overlay of (a) kaempferol and (b) kaempferol stabilized gold nanoparticle, KAunp.

intact in KAunp indicating presence of stabilizing kaempferol molecules. It was likely that some of the kaempferol phenolic O–H groups were responsible for gold nanoparticles stabilization in solution. Similar observations were recorded in case of other bioflavonoids stabilized gold nanoparticles.[31]

3.3. Antileishmanial activity and cytotoxicity

The highly stable monodispersed KAunp, kaempferol, SSG and PMM were tested parallely for antileishmanial efficacy in the macrophages. Both the axenic amastigotes and the intra cellular forms were treated with all compounds (Table 1). Amphotericin B was highly potent but cytotoxic in nature. Kaempferol alone was effective against the wild *L. donovani* parasite strains but that effect was not as pronounced as in case of SSG or PMM treatment. Intracellular amastigotes appeared more sensitive to the nanoparticles exposure. In the wild type parasite strains, KAunp IC_{50} was recorded as 4 ± 0.6 μM in axenic amastigotes while that in microphage infested condition was at 3 ± 0.5 μM. Toxic manifestation for KAunp was lowest among all the test compounds; CC_{50} in microphages was recorded at 2.4×10^2 μM. Kaempferol is a flavonoid.

Similar bio-active molecules from plant sources were investigated earlier in a search for alternative antileishmanial chemotherapeautics.[32] Flavonoids antiprotozoal activity is generally linked to the reactive oxygen species (ROS) generations, intense vacualization, inhibition of energy metabolism and mitochondrial membrane disruption.[33] *In silico* modelling and gene cloning experiments in *E. coli* very recently indicated that kaempferol can be one alternative chemotherapeutic in leishmaniasis.[34] When we studied kaempferol against the drug resistant and wild type *L. donovani* strains the compound appeared potent in all cases. Kaempferol IC_{50} against the SSG resistant axenic amastigotes was 30 ± 5 μM while that in case of macrophage infested amastigotes were 25 ± 3 μM. The selectivity index (SI) indicate parasite knockout effects compared to toxicity. Kaempferol SI against wild type macrophage infested amastigote was lower than either SSG PMM or amphotericin B. The resistance index (RI) for kaempferol was lower in resistance strains indicating somewhat nonspecific efficacy and low macrophage toxicity. It was interesting to note that KAunp was effective against both wild and drug resistant strains. The SI parameter for KAunp was lower than amphotericin B but the RI parameter was convincingly higher in SSG and PMM resistant strains. It was therefore imperative that the KAunps are relatively safe but encouragingly effective against both the wild and drug resistant *L. donovani* strains. Gold compounds have attracted attention in recent times for profound antileishmanial efficacy expressions. The anti-inflammatory gold compound Auranofin for example was effective in parasite infection control due to thiol redox enzyme inhibition effects.[35,36] However, unlike the gold nanoparticles the metal–

Table 1 *In vitro* antileishmanial activity of kaempferol, KAunp and standard drugs on axenic and intracellular amastigotes of *Leishmania donovani* and drug resistant cell lines[a]

Drug	IC_{50} (mean ± SD for 3 replicates)[b] μM								Cytotoxicity CC_{50} (μM) (macrophage cells)
	WT	SI[c]	SSG resistant	RI[d]	SI[c]	PMM resistant	RI[d]	SI[c]	
Axenic amastigote									
Amphotericin B	0.2 ± 0.05^e	70	0.4 ± 0.05^e	2	35	0.35 ± 0.05^e	1.75	40	
Sodium stibogluconate (SSG)	3.6 ± 0.40	7.5	130 ± 20	36	0.20	115 ± 16	32	0.23	
Paromomycin (PMM)	10 ± 2^e	25	380 ± 40^e	38	0.65	330 ± 30^e	33	0.75	
Kaempferol	25 ± 4^e	8	30 ± 5^e	1.20	6.67	48.2 ± 9^e	1.93	4.15	
KAunp	4 ± 0.6^f	60	4.5 ± 1.3^e	1.12	53.33	5.3 ± 1.6^e	1.33	45.28	
Amastigote in macrophage									
Amphotericin B	0.15 ± 0.05^e	93	0.2 ± 0.05^e	1.33	70	0.18 ± 0.05^e	1.20	78	14
Sodium stibogluconate (SSG)	1.6 ± 0.2	17	18.1 ± 3	11.25	1.5	17.3 ± 2.6	10.81	1.6	27
Paromomycin (PMM)	8 ± 2^e	31	125 ± 15^e	15.63	2	115 ± 13^e	14.38	2.1	248
Kaempferol	20 ± 5^e	10	25 ± 3^e	1.25	8	42.6 ± 7.3^e	2.13	4.69	2×10^2
KAunp	3.0 ± 0.5^e	80	3.6 ± 1^e	1.20	66.67	5 ± 1.4^e	1.67	48	2.4×10^2

[a] WT (Wild Type), SSG (sodium stibogluconate resistant) and PMM (paromomycin) resistant lines. [b] Results expressed as mean ± SD ($n = 3$). [c] Selectivity Index (SI) was calculated by dividing the CC_{50} by IC_{50}. [d] Resistance Index (RI) was calculated by dividing the IC_{50} for resistant parasites by that for WT parasites. [e] $P < 0.05$ significant difference compared with SSG. [f] $P < 0.5$ no significant difference compared with SSG.

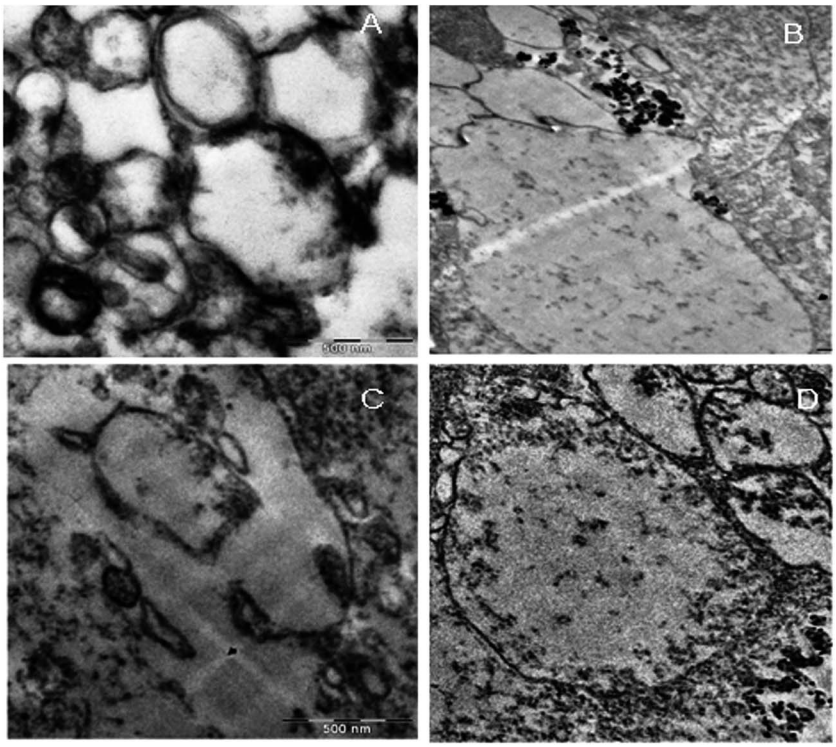

Fig. 7 Nanoparticles cellular uptake studies in TEM. The nanoparticles treated macrophages were observed at different time intervals. (A) Macrophages without KAunp exposure, (B) after 10 min exposure, (C) after 30 min exposure, and (D) after 1 h exposure.

organic complexes are unstable in physiological environment. We have proposed gold nanoparticles design earlier for effective control of parasite infections.[37] KAunps profound efficacy against macrophage infested *L. donovani* strains was likely due to thiol redox enzyme inhibition and kaempferol inhibition of parasite pyrimidine biosynthesis pathways. Highly specific uptake by the macrophages and minimal toxicity added another advantage for newly designed gold nanoparticles in control of macrophage cell resident *L. donovani* infections.

On the other hand, metal nanoparticles are able to produce high amount of ROS in a nonenzymatic way which can induce oxidative stress leading to DNA damage and alkylation of target proteins and ultimately apoptosis of the parasite. Several metal nanoparticles such as selenium nanoparticles, antimony sulfide NPs (Sb_2S_5) and silver nanoparticles evaluated for their *in vitro* and *in vivo* activity against *Leishmania* spp.[38–40] Recent studies have demonstrated enzymes consist of free thiol-containing active sites may interact with metal ions and selectively inhibited. Trypanothione reductase ($T(SH)_2$) enzyme associated in the *Leishmania* metabolism and cysteine proteases such as cathepesin L-like or cathepsin B-like were identified as a primary targets to metal nanoparticles.[41,42] According to our view, the improvement of antileishmanial efficacy of the KAunp attributed due to metal–drug synergism approach and may consider as alternative drug design at this point. Parasitic protozoan like *Leishmania* are susceptible to redox biology fluctuations and KAunp likely induced dramatic redox stress and nuclear damage in macrophage resident infection conditions.

3.4. Macrophage uptake studies

KAunp interactions with the macrophages were observed in TEM studies at a 75 kV exposure. Nanoparticles assimilation and internalization appeared as a function of exposure time. Fig. 7 presented TEM observations studies. The accumulation of nanoparticles into the cells increased with incubation time and maximum uptake observed less than 2 h of exposure. Macrophage infiltration was visualized around 30 min exposure time. Before that event nanoparticles accumulated closer to the cell membrane and a significant number of KAunp uptake was observed after 1 h of incubation. Nanoparticle surface charge and spherical shape should be some of the reasons for almost no membrane damage. This data could be correlated clearly with the low toxicity observations due to KAunp.

4. Conclusion

We report highly monodispersed spherical gold nanoparticles (KAunp) synthesis using kaempferol as one *in situ* reductant and stabilizer. Rapid reduction, nucleation and nanoparticles growth culminated in homogeneous gold sol ~18.2 nm in diameter. *L. donovani* is a life threatening macrophage resident NTD infection. Drug resistance in leishmaniasis is rampant and new drug development has remained mostly ignored. A crying need therefore exists for alternate chemotherapy strategy for control of leishmaniasis. We proposed KAunp as a successful alternative for control of wild and drug resistant *L. donovani* strains. KAunp invaded infected macrophages within 1 h of

exposure and induced parasite knockout. The gold nanoparticles also appeared as a safer alternative to SSG and PMM.

Acknowledgements

AH would like to thank the UGC for URF fellowship grants (Sanction No: UGC/312/Fellow (Univ.), dated: 07.04.2015). SD would like to thank UGC for Post Doctoral Fellowship for Women (Sanction No: F.15-1/2015-16/PDFWM-2015-17-WES-33815 (SA-II). Thanks are also due to Dr Nahid Ali and Prof. Ashish Sen (Jr) of Indian Institute for Chemical Biology, Kolkata, India for the nanoparticles macrophage uptake studies.

References

1 K. Niikura, N. Iyo, Y. Matsuo, H. Mitomo and K. Ijiro, *ACS Appl. Mater. Interfaces*, 2013, **5**, 3900.
2 H. Herd, N. Daum, A. T. Jones, H. Huwer, H. Ghandehari and C.-M. Lehr, *ACS Nano*, 2013, **7**, 1961.
3 L. Treuel, X. Jiang and G. U. Nienhaus, *J. R. Soc., Interface*, 2013, **10**, 1.
4 E. C. Dreaden, M. A. Mackey, X. Huang, B. Kangy and M. A. El-Sayed, *Chem. Soc. Rev.*, 2011, **40**, 3391.
5 B. D. Chithrani, A. A. Ghazani and W. C. Chan, *Nano Lett.*, 2006, **6**, 662.
6 S. Mukherjee, B. Vinothkumar, S. Prashanthi, P. R. Bangal, B. Sreedhar and C. R. Patra, *RSC Adv.*, 2013, **3**, 2318.
7 B. Đ. Glišić and M. I. Djuran, *Dalton Trans.*, 2014, **43**, 5950.
8 P. Narayanasamy, B. L. Switzer and B. E. Britigan, *Sci. Rep.*, 2015, **5**, 1.
9 J. d. Neves, M. M. Amiji, M. F. Bahia and B. Sarmento, *Adv. Drug Delivery Rev.*, 2010, **62**, 458.
10 B. J. Edagwa, D. Guo, P. Puligujja, H. Chen, J. McMillan, X. Liu, H. E. Gendelman and P. Narayanasamy, *FASEB J.*, 2014, **28**, 5071.
11 S. D. Perrault and W. C. W. Chan, *J. Am. Chem. Soc.*, 2009, **131**, 17042.
12 S. J. Hwang, S. H. Jun, Y. Park, S.-H. Cha, M. Yoon, S. Cho, H.-J. Lee and Y. Park, *Nanomedicine*, 2015, **11**, 1677.
13 J. Turkevich, P. C. Stevenson and J. Hillier, *Discuss. Faraday Soc.*, 1951, **11**, 55.
14 R. K. Mathur, A. Awasthi, P. Wadhone, B. Ramanamurthy and B. Saha, *Nat. Med.*, 2004, **10**, 540.
15 R. García-Hernańdez, J. I. Manzano, S. Castanys and F. Gamarro, *PLoS Neglected Trop. Dis.*, 2012, **6**, e1974.
16 V. Bhandari, S. Sundar, J. C. Dujardin and P. Salotra, *Antimicrob. Agents Chemother.*, 2014, **58**, 2585.
17 P. D. Gianvincenzo, M. Marradi, O. M. Martínez-Ávila, L. M. Bedoya, J. Alcamí and S. Penadés, *Bioorg. Med. Chem. Lett.*, 2010, **20**, 2718.
18 A. K. Ghosh, F. K. Bhattacharyya and D. K. Ghosh, *Exp. Parasitol.*, 1985, **60**, 404.
19 D. Sereno and J. L. Lemesre, *Antimicrob. Agents Chemother.*, 1997, **41**, 972.
20 H. L. Callahan, C. Kelley, T. Pereira and M. Grogl, *Antimicrob. Agents Chemother.*, 1996, **40**, 947.
21 K. P. Chang, *Science*, 1980, **209**, 1240.
22 P. Nativo, I. A. Prior and M. Brust, *ACS Nano*, 2008, **2**, 1639.
23 J. Piella, N. G. Bastús and V. Puntes, *Chem. Mater.*, 2016, **28**, 1066.
24 N. G. Bastus, J. Comenge and V. Puntes, *Langmuir*, 2011, **27**, 11098.
25 L. V. Jørgensen, C. Cornett, U. Justesen, L. H. Skibsted and L. O. Dragsted, *Free Radical Res.*, 1998, **29**, 339.
26 G. Frens, *Nature, Phys. Sci.*, 1973, **241**, 20.
27 E. Gachard, H. Remita, J. Khatouri, B. Keita, L. Nadjo and J. Belloni, *New J. Chem.*, 1998, **22**, 1257.
28 D. Radziuk, D. Shchukin and H. Molhwald, *J. Phys. Chem. C*, 2008, **112**, 2462.
29 V. Butkovicä, L. Klasinc and W. Bors, *J. Agric. Food Chem.*, 2004, **52**, 2816.
30 L. Bellamy, *The Infrared Spectra of Complex Molecules*, Springer, London, 1975.
31 L. A. Levchenko, S. A. Golovanova, N. V. Lariontseva, A. P. Sadkov, D. N. Voilov, Y. M. Shul'ga, N. G. Nikitenko and A. F. Shestakov, *Russ. Chem. Bull.*, 2011, **60**, 426.
32 D. Tasdemir, M. Kaiser, R. Brun, V. Yardley, T. J. Schmidt, F. Tosun and P. Rüedi, *Antimicrob. Agents Chemother.*, 2006, **50**, 1352.
33 C. Marîn, S. Boutaleb-Charki, J. G. Dîaz, O. Huertas, M. J. Rosales, G. Pérez-Cordon, R. Guitierrez-Sánchez and M. Sánchez-Moreno, *J. Nat. Prod.*, 2009, **72**, 1069.
34 K. Tiwari, R. Kumar and V. K. Dubey, *Biochimie*, 2016, **131**, 45.
35 E. R. Sharlow, S. Leimgruber, S. Murray, A. Lira, R. J. Sciotti, M. Hickman, T. Hudson, S. Leed, D. Caridha, A. M. Barrios, D. Close, M. Grögl and J. S. Lazo, *ACS Chem. Biol.*, 2014, **9**, 663.
36 M. T. A. da Silva, I. Silva-Jardim, G. B. Portapilla, G. M. Alvares de Lima, F. C. Costa, F. D. F. Anibal and O. H. Thiemann, *Exp. Parasitol.*, 2016, **166**, 189.
37 S. Das, P. Roy, S. Mondal, T. Bera and A. Mukherjee, *Colloids Surf., B*, 2013, **107**, 27.
38 N. Beheshti, S. Soflaei, M. Shakibaie, M. H. Yazdi, F. Ghaffairfar, A. Dalimi and A. R. Shahverdi, *J. Trace Elem. Med. Biol.*, 2013, **27**, 203.
39 S. Soflaei, A. Dalimi, F. Ghaffarifar, M. Shakibaie, A. R. Shahverdi and M. Shafiepour, *J. Parasitol. Res.*, 2012, DOI: 10.1155/2012/756568.
40 A. M. Allahverdiyev, E. S. Abamor, M. Bagirova, C. B. Ustundag, C. Kaya, F. Kaya and M. Rafailovich, *Int. J. Nanomed.*, 2011, **6**, 2705.
41 Ashutosh, S. Sundar and N. Goyal, *J. Med. Microbiol.*, 2007, **56**, 143.
42 S. P. Fricker, *Metallomics*, 2010, **2**, 366.